UC San Diego

UC San Diego Previously Published Works

Title

Using Noble Gas Measurements to Derive Air-Sea Process Information and Predict Physical Gas Saturations

Permalink

https://escholarship.org/uc/item/9n74j0h1

Journal

Geophysical Research Letters, 44(19)

ISSN

0094-8276

Authors

Hamme, Roberta C
Emerson, Steven R
Severinghaus, Jeffrey P
et al.

Publication Date

2017-10-16

DOI

10.1002/2017gl075123

Peer reviewed

eScholarship.org Powered by the California Digital Library
University of California

AGU PUBLICATIONS

Geophysical Research Letters

RESEARCH LETTER
10.1002/2017GL075123

Key Points:
- Physical processes at the air-sea interface during water-mass formation can be quantified from noble gas measurements
- Process rates derived from noble gases can be used to predict the expected physically forced concentration of other gases
- Physical processes likely supersaturate SF_6 by ~6% relative to CFC-11 and CFC-12 in the Labrador Sea

Supporting Information:
- Supporting Information S1

Correspondence to:
R. C. Hamme,
rhamme@uvic.ca

Citation:
Hamme, R. C., Emerson, S. R., Severinghaus, J. P., Long, M. C., & Yashayaev, I. (2017). Using noble gas measurements to derive air-sea process information and predict physical gas saturations. *Geophysical Research Letters*, *44*, 9901–9909.
https://doi.org/10.1002/2017GL075123

Received 28 JUL 2017
Accepted 7 SEP 2017
Accepted article online 13 SEP 2017
Published online 12 OCT 2017

©2017. American Geophysical Union. All Rights Reserved.

Using Noble Gas Measurements to Derive Air-Sea Process Information and Predict Physical Gas Saturations

Roberta C. Hamme[1], Steven R. Emerson[2], Jeffrey P. Severinghaus[3], Matthew C. Long[4], and Igor Yashayaev[5]

[1]School of Earth and Ocean Sciences, University of Victoria, Victoria, British Columbia, Canada, [2]School of Oceanography, University of Washington, Seattle, WA, USA, [3]Scripps Institution of Oceanography, University of California, San Diego, La Jolla, CA, USA, [4]Climate and Global Dynamics Division, National Center for Atmospheric Research, Boulder, CO, USA, [5]Fisheries and Oceans Canada, Bedford Institute of Oceanography, Dartmouth, Nova Scotia, Canada

Abstract Dissolved gas distributions are important because they influence oceanic habitats and Earth's climate, yet competing controls by biology and physics make gas distributions challenging to predict. Bubble-mediated gas exchange, temperature change, and varying atmospheric pressure all push gases away from equilibrium. Here we use new noble gas measurements from the Labrador Sea to demonstrate a technique to quantify physical processes. Our analysis shows that water-mass formation can be represented by a quasi steady state in which bubble fluxes and cooling push gases away from equilibrium balanced by diffusive gas exchange forcing gases toward equilibrium. We quantify the rates of these physical processes from our measurements, allowing direct comparison to gas exchange parameterizations, and predict the physically driven saturation of other gases. This technique produces predictions that reasonably match N_2/Ar observations and demonstrates that physical processes should force SF_6 to be ~6% more supersaturated than CFC-11 and CFC-12, impacting ventilation age calculations.

Plain Language Summary Gases dissolved in the ocean are important because they influence oceanic habitats and Earth's climate. Physics and biology combine to control the amounts of gases like carbon dioxide, oxygen, and nitrogen in the ocean. Our research seeks to disentangle and quantify the competing effects of physics and biology on dissolved gases. We present very precise measurements of dissolved noble gas concentrations (neon, argon, and krypton) in the Labrador Sea, one of the few places on Earth where the surface and deep ocean communicate with each other. Because noble gases have no biological function, responding only to physical processes in the ocean, we use these measurements to discover the amounts of physical processes that affect gases during the winter at this site, like rapid cooling of the water or bubbles injected by breaking waves. From these amounts of physical processes, we calculate the concentrations of nitrogen and chlorofluorocarbons if only physical processes affected these gases. Our work will allow oceanographers to better estimate the rate that bioavailable nutrients are being removed from the ocean (a process that biologically creates nitrogen gas) and to better determine how the ocean moves from observations of changing chlorofluorocarbons in the ocean.

1. Introduction

Observations of dissolved gases in the ocean can be used to quantify processes from biological production to ventilation and mixing. Both physical and biological processes drive oxygen, nitrogen, and carbon concentrations. If the influences of physics and biology can be separated, net community production rates can be derived from oxygen distributions and denitrification rates from nitrogen (e.g., Chang et al., 2012; Hamme & Emerson, 2006). Physical processes also control the carbon solubility pump, so constraints on these processes are needed to assess model ventilation (Nicholson et al., 2010, 2016; Toggweiler et al., 2003). Using chlorofluorocarbons (CFCs) to quantify the ventilation age of thermocline waters requires accurate estimates of their surface concentrations during subduction (e.g., Stöven et al., 2016), also driven by physical air-sea exchange processes.

Physical processes at the air-sea interface can be quantified using noble gases, which are biologically inactive and have constant dry atmospheric concentrations (Stanley & Jenkins, 2013). Their different solubilities,

temperature dependencies, and diffusivities force each to respond differently to bubble dissolution, temperature changes, and gas exchange. The groundwater community has long used noble gases to quantitatively separate physical processes, especially to derive paleotemperatures (e.g., Aeschbach-Hertig et al., 2000; Stute et al., 1992). Ocean measurements have been used to develop air-sea gas exchange parameterizations (Stanley et al., 2009), to determine glacial meltwater fractions (Hohmann et al., 2002; Loose et al., 2016), and to correct oxygen-based estimates of productivity rates (e.g., Spitzer & Jenkins, 1989). Here, using noble gas measurements from the Labrador Sea, we develop a technique to quantify air-sea interactions and predict physically driven saturations of other gases.

2. Methods

Sampling was conducted on the AR7W hydrographic line across the Labrador Sea in May 2007, 2011, 2015, and 2016 and from an August 2015 GEOTRACES cruise. Noble gases from 2007 were analyzed at Scripps Institution of Oceanography (SIO) following Hamme and Severinghaus (2007) with no Ne analyses, while the rest were analyzed at University of Victoria (UVic) following a similar method. Briefly, duplicate water samples were collected into preevacuated 180 mL glass flasks until half full. Starting in 2011, samples were vacuum preserved at sea and in the lab by connecting the flask necks to a vacuum pump. Back in the lab, flasks were weighed and the water extracted after equilibration with the headspace. Headspace gases were purified through a trap at −85°C, gettered to remove all gases except noble gases, mixed with ^{38}Ar for isotope dilution and a balance gas of either N_2 (2007) or He (2011–2016), and analyzed for Ar isotopes and Ne/Ar/Kr ratios on a dual-inlet isotope-ratio mass spectrometer. Samples from 2015 AR7W were not properly vacuum preserved, resulting in >1.5% higher Ne than other results, so we excluded them. From comparison to previous data, Ar and Kr do not appear affected, likely because these gases have lower diffusivities (Sturm et al., 2004). We display these 2015 Ar and Kr data but do not perform quantitative calculations with them. The pooled standard deviations of the duplicates in this data set were 0.31% for Ne, 0.09% for Ar, and 0.12% for Kr. We excluded samples without duplicates or for which the duplicate standard deviation exceeded 3 times the pooled standard deviation.

We collected separate samples for N_2/Ar ratio measurements on the 2007–2015 cruises in a similar manner. Samples from 2011 to 2015 were cryogenically purified through liquid N_2 and analyzed by mass spectrometry (Emerson et al., 1999; Hamme & Emerson, 2013). Values were corrected for oxygen content differences between sample and standard based on standards with known O_2/N_2/Ar ratios. Most 2011 samples were analyzed at University of Washington, while some 2011 and all 2015 samples were analyzed at UVic, with no detectable offsets. Samples from 2007 were purified with heated copper to remove oxygen and analyzed at SIO (Kobashi et al., 2008). For 2011–2015 samples, the pooled standard deviation of N_2/Ar duplicates was 0.078%. We excluded samples without duplicates or for which the duplicate standard deviation exceeded 3 times 0.074%. We show 2007 samples, despite not being collected in duplicate, because the excellent reproducibility between methods points to low bias.

Because these gas concentrations are close to equilibrium and that deviation contains the key information, we present the data as the saturation anomaly; for example,

$$\Delta\mathrm{Ne} = \frac{[\mathrm{Ne}]_{\mathrm{meas}}}{[\mathrm{Ne}]_{\mathrm{equil}}} - 1, \tag{1}$$

where ΔNe is graphically displayed in percent (×100), $[\mathrm{Ne}]_{\mathrm{meas}}$ is the measured Ne concentration, and $[\mathrm{Ne}]_{\mathrm{equil}}$ is the Ne concentration at equilibrium with 1 atm pressure for the potential temperature and salinity of the water (Bullister et al., 2002; Hamme & Emerson, 2004; Warner & Weiss, 1985; Weiss & Kyser, 1978). We present the saturation anomaly for the gas ratio N_2/Ar similarly with (N_2/Ar) replacing Ne in equation (1) (Hamme & Emerson, 2013).

We interpret our results using both a simple mixed-layer model and an Earth system model. The mixed-layer model incorporates seasonal cooling and air-sea gas exchange in a single layer with constant depth. The Community Earth System Model (CESM), version 1.2, simulates inert gases in a three-dimensional ocean general circulation model based on POP2 (Long et al., 2016) (supporting information). It computes air-sea gas exchange following Wanninkhof (1992) with an additional small bubble flux following Ito et al. (2011). Gas tracers were initialized using a Newton-Krylov technique for accelerating spin-up (Lindsay, 2017).

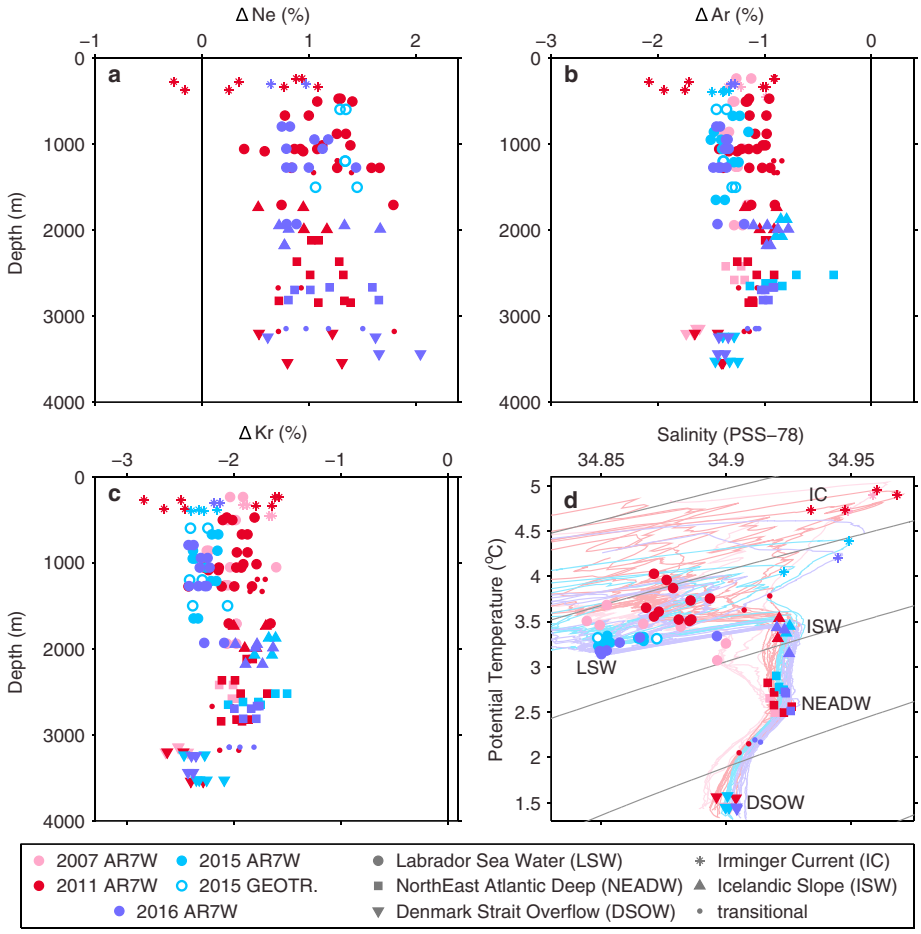

Figure 1. Depth profiles of (a) neon, (b) argon, and (c) krypton saturation anomalies (%) in the Labrador Sea. Color indicates cruise and year, while shape indicates water mass. *X* axis range is 3.4% in all three panels. Measurements shallower than 200 m excluded. (d) Symbols show potential temperature (°C) versus salinity (PSS-78) for these samples, while lines show full profiles from the same casts.

3. Observations

The noble gases show consistent patterns in Labrador Sea deep waters. Neon is supersaturated, while argon and krypton are undersaturated (Figure 1). Several deep water masses exist here: Labrador Sea Water formed by local deep convection, as well as Icelandic Slope Water and NE Atlantic Deep Water characterized by deep salinity maxima and Denmark Strait Overflow Water at the bottom with a temperature minimum, all three of which form by convection and mixing outside the Labrador basin (Yashayaev, 2007). There are small differences in noble gases between these waters, with argon and krypton tending to be lowest in Denmark Strait Overflow Water and highest in Icelandic Slope Water and NE Atlantic Deep Water. Neon does not show this pattern, perhaps because of lower analytical precision. We also sampled Irminger Current water in the boundary current around SW Greenland. This shallower water mass (~400 m) convectively formed in the Irminger Sea (Yashayaev, 2007) has lower saturation anomalies for all three gases. Although we collected samples in spring and summer, measured saturation anomalies should represent the end of winter convection when the water is isolated from atmospheric interaction. Yashayaev and Loder (2016) show that salinity and temperature evolve only slightly in Labrador Sea Water from the end of convection to summer, and we detect no changes between our spring and summer 2015 cruises.

4. Impact of Physical Processes on Noble Gases

Physical processes push noble gas saturation anomalies away from equilibrium by different amounts depending on gas properties. This allows noble gases to serve as quantitative tracers of atmospheric pressure variation, temperature change, and bubble-mediated gas exchange (Figure 2).

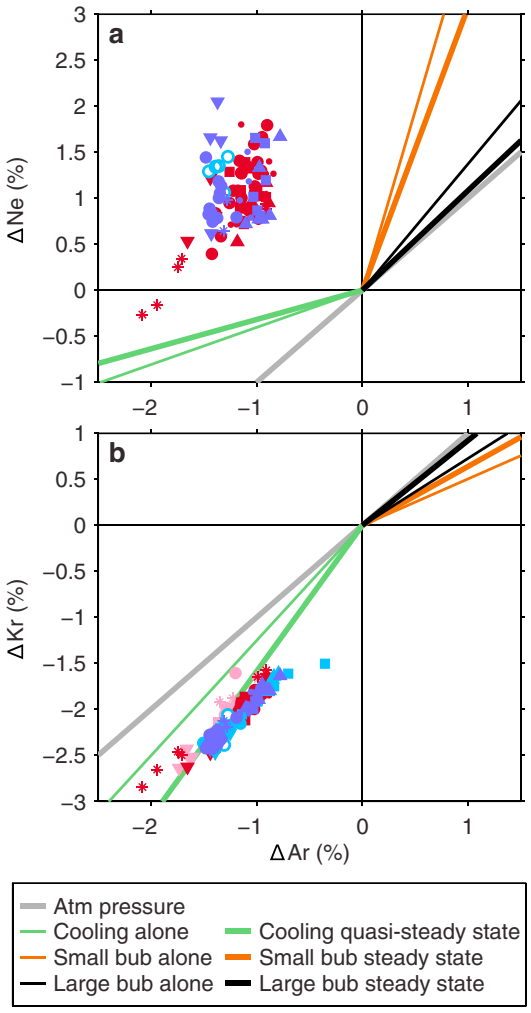

Figure 2. Vectors showing the expected impact of different processes on (a) neon versus argon saturation anomaly and (b) krypton versus argon saturation anomaly. Lines show the direction a given process would force gas saturation anomalies away from equilibrium (the origin). Symbols show same data as Figure 1.

First, gas saturation anomalies are calculated with respect to equilibrium with an atmospheric pressure of 1 atm. In regions like the Labrador Sea, mean winter atmospheric pressures are lower. When gases equilibrate with lower atmospheric pressures, their calculated saturation anomalies appear lower but all by the same amount, so atmospheric pressure variation affects gases in a 1:1 ratio (Figure 2, gray lines).

Second, temperature change affects saturation anomalies through changing the expected equilibrium concentration, not the actual concentration. Gases are more soluble in cold water, with Ne having the least temperature sensitivity and Kr the most. Therefore, cooling draws down Kr saturation anomalies more strongly than Ar and Ar more strongly than Ne. Cooling alone moves gas saturation anomalies along the thin green lines in Figure 2. However, as cooling occurs, diffusive gas exchange at the air-sea interface brings gas saturation anomalies back toward equilibrium. When these processes balance, a quasi steady state occurs as cooling draws down saturation anomalies at the same rate that diffusive gas exchange increases them. Neon with the highest diffusivity is driven toward equilibrium more rapidly, while Kr with the lowest diffusivity is affected less; this effect changes the cooling line slope for a quasi steady state to the thick green lines in Figure 2.

Third, breaking waves push air bubbles beneath the surface, where higher pressure encourages dissolution. Small dissolving bubbles strongly increase the saturation anomaly of low-solubility gases, because there is relatively little of these gases already present in the water (Craig & Weiss, 1971; Hamme & Severinghaus, 2007). Neon is least soluble and Kr most soluble, so small bubbles increase Ne saturation anomalies relative to Ar and Ar relative to Kr (Figure 2, thin orange lines). Again, diffusive gas exchange acts to return gases toward equilibrium. A steady state is reached when small bubble dissolution increases gas concentrations at the same rate that diffusive gas exchange decreases them, changing the small bubble slope for a steady state to the thick orange lines in Figure 2. Fluxes of gases from large bubbles that exchange only a portion of their gases with the water before returning to the surface are less affected by gas solubility and more by diffusivity. In Figure 2, we demonstrate their effect in the black lines based on the Liang et al. (2013) parameterization. At steady state, the effect of large bubbles (thick black lines) is nearly indistinguishable from higher atmospheric pressure.

Finally, several processes that affect noble gas saturation anomalies in other locations are likely not significant in the central Labrador Sea. Glacial ice melt is important to explaining noble gas signatures in the Southern Ocean (Hohmann et al., 2002; Loose et al., 2016) and in glacial fjords (Beaird et al., 2015). Sea ice formation affects gases by partitioning gases among bubbles, ice, and brine (Postlethwaite et al., 2005). However, waters in the central Labrador Sea form by open ocean convection, with glacial and sea ice melt largely confined to the boundary currents (Myers, 2005). Meltwater that makes its way to the center does so at the surface, where gas exchange erases its signature. Because equilibrium concentrations of noble gases are curved functions of temperature, mixing between waters of very different temperature increases gas saturation anomalies (Emerson et al., 2012; Ito & Deutsch, 2006). During deep convection, the water brought into the mixed layer has a similar temperature, so that vertical mixing should not significantly increase gas saturation anomalies by this mechanism.

5. Quantifying Physical Processes

We next calculate the amount of each process necessary to explain the observations. No one process explains our data, because no single process causes both Ne supersaturation and Ar undersaturation (Figure 2). Instead, we consider a combination of processes in a mixed-layer model, with two cases excluding or including diffusive gas exchange. Hamme and Emerson (2002) showed that diffusive gas exchange acting to return gases

toward equilibrium is needed to explain oceanic inert gas saturation anomalies. However, recent papers have interpreted noble gas data without this effect (Loose et al., 2016), so we evaluate both approaches.

Our mixed-layer model interacts with the atmosphere but does not entrain or mix with other waters. This framework avoids assumptions for subsurface gas concentrations but oversimplifies a deeply convecting site. The drawbacks of this practical approach are reduced in the Labrador Sea, where the previous winter's convection produces a relatively homogeneous water mass, reducing the impact of vertical exchange. In fact, our observations of Labrador Sea Water represent the integrated effect of multiple winters' convection, such that the time scale for surface fluxes to act on the water mass is longer than a single winter.

In the first case, we exclude diffusive gas exchange, following Loose et al. (2016) but with the addition of large bubbles. The saturation anomaly of a generic gas, C, that begins at equilibrium with a specific atmospheric pressure and large bubble overpressure and then is pushed away from equilibrium by constant rates of cooling and small bubble dissolution is as follows:

$$\Delta C = \left\{ \frac{P_{\mathrm{SLP}}}{P_{\mathrm{ATM}}} - 1 + \Delta P \right\} + \left\{ -\frac{\mathrm{d}T}{\mathrm{d}t}\delta t \right\} \left(\frac{\mathrm{d}[C]_{\mathrm{equil}}}{\mathrm{d}T} \frac{1}{[C]_{\mathrm{equil}}} \right) + \left\{ \frac{k_c \delta t}{h} \right\} \left(\frac{\chi_C}{[C]_{\mathrm{equil}}} \right), \tag{2}$$

where ΔC is the saturation anomaly (equation (1)), $P_{\mathrm{SLP}}/P_{\mathrm{ATM}}$ is the ratio of sea level pressure to standard atmospheric pressure (unitless), $\mathrm{d}T/\mathrm{d}t$ is the rate of temperature change (°C s^{-1}), δt is the change in time (s), k_C is the rate of small bubble air dissolution (mol m^{-2} s^{-1}) and should depend heavily on wind speed, h is the surface layer depth (m), and χ_C is the atmospheric mole fraction (see the supporting information for a derivation). We represent large bubbles as an average fractional overpressure in the bubbles, ΔP (unitless). This implies that large bubbles affect each gas identically, which is not strictly true. However, large bubbles and atmospheric pressure are similar in their effects (Figure 2), so we combine them. The terms in curly braces are gas independent, whereas the terms in rounded parentheses combine all gas-dependent terms such as solubility and atmospheric mole fraction. The ratio of the terms in parentheses define the slopes of the thin lines in Figure 2. Writing equation (2) for each of our three gases, we solve for the three gas-independent terms in curly braces.

In the second case, we include diffusive gas exchange in our mixed-layer model as a flux parameterized by $k_s([C]_{\mathrm{equil}} \frac{P_{\mathrm{SLP}}}{P_{\mathrm{ATM}}} - C)$. We follow Emerson and Bushinsky (2016) to solve for a quasi steady state where cooling and bubble fluxes pushing gases away from equilibrium are balanced by diffusive gas exchange pushing gases back toward equilibrium, such that surface gas saturation anomalies are relatively constant. Following Liang et al. (2013), we parameterize large bubble fluxes as $k_p((1 + \Delta P)[C]_{\mathrm{equil}} - [C])$, except we assume k_p has a 0.5 dependence on the Schmidt number rather than 0.67, which simplifies the final equation.

$$\begin{aligned} \Delta C = & \left\{ \frac{P_{\mathrm{SLP}}}{P_{\mathrm{ATM}}} - 1 + \frac{\Delta P k_{p,660}}{k_{s,660} + k_{p,660}} \frac{P_{\mathrm{SLP}}}{P_{\mathrm{ATM}}} \right\} \\ & + \left\{ h \frac{P_{\mathrm{SLP}}}{P_{\mathrm{ATM}}} \frac{\mathrm{d}T}{\mathrm{d}t} \left(\frac{1}{k_{s,660} + k_{p,660}} + \frac{\Delta P k_{p,660}}{\left(k_{s,660} + k_{p,660}\right)^2} \right) \right\} \left(-\left(\frac{Sc}{660} \right)^{0.5} \frac{\mathrm{d}[C]_{\mathrm{equil}}}{\mathrm{d}T} \frac{1}{[C]_{\mathrm{equil}}} \right) \\ & + \left\{ \frac{k_c}{k_{s,660} + k_{p,660}} \right\} \left(\left(\frac{Sc}{660} \right)^{0.5} \frac{\chi_C}{[C]_{\mathrm{equil}}} \right), \end{aligned} \tag{3}$$

where $k_{s,660}$ is the diffusive gas transfer velocity for a gas with Schmidt number 660 (m s^{-1}), $k_{p,660}$ is the large bubble gas transfer velocity for Schmidt number 660 (m s^{-1}), and Sc is the gas's Schmidt number (see the supporting information). The ratio of the terms in parentheses defines the slope of the thick lines in Figure 2. Again, writing equation (3) for each of our three gases, we solve for the terms in curly braces.

The first case with equation (2), which excludes diffusive gas exchange, yields atmospheric pressure plus large bubble overpressures of 2.1% above one atmosphere (+2.1 ± 0.7 %), wintertime cooling of −1.4 ± 0.2°C, and essentially no small bubble-induced flux (0.002 ± 0.003 mol m^{-3}) (Figure 3). Conversely, the second case, including the effects of diffusive gas exchange in a quasi steady state, yields atmospheric pressures plus large bubble overpressures of 1.0% below 1 atm (−1.0 ± 0.3%), cooling of −0.35 ± 0.06 °C, and a small bubble contribution of 0.010 ± 0.002 mol m^{-3}. Observed wintertime atmospheric pressures in the Labrador Sea convection region are below 1 atm: −1.3% in January to −0.5% in March (1981–2010 National Centers for Environmental Prediction (NCEP) reanalysis (Kalnay et al., 1996)), which is clearly closer to the model that includes diffusive gas exchange. Measured wintertime temperature changes are about −4°C, which is a larger decrease

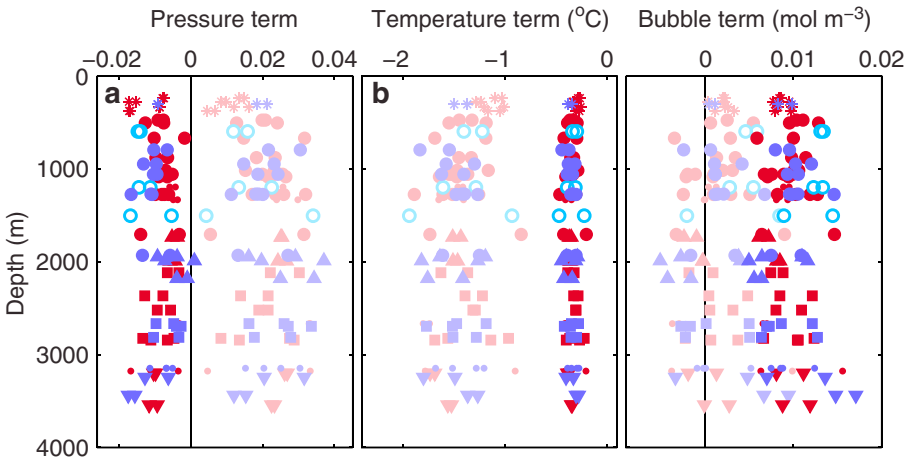

Figure 3. Solutions for gas-independent terms causing saturation anomalies from 2011 and 2016 AR7W and 2015 GEOTRACES noble gas data. Symbols indicate cruise and water mass. Lighter colors indicate the first case excluding diffusive gas exchange (equation (2)), while darker colors indicate the second case including diffusive gas exchange (equation (3)). Each panel plots the terms in curly braces in these equations, so the two solutions are not directly comparable. (a) Contribution of atmospheric pressure and large bubble overpressure (unitless), (b) contribution of temperature change (°C), and (c) contribution of small bubbles (mol m^{-3}).

than either model estimate, but the temperature terms enclosed in the curly braces of equation (3) include more than just temperature change, so it is not appropriate to compare this result with that of equation (2) or with the observations.

We judge how realistic the noble gas derived small bubble fluxes are by comparing Figure 3c with the wind speed-dependent parameterization of Liang et al. (2013). Using 2006–2015 6 h Cross-Calibrated Multi-Platform v2 10 m wind speeds (CCMPv2) (Atlas et al., 2011), we calculated the wind speed frequency distribution for each winter month in the Labrador Sea convective region. We then calculated the small bubble term, $k_c/(k_{s,660} + k_{p,660})$, using the Liang et al. (2013) parameterization at each wind speed and summed the contributions over the frequency distributions to arrive at an average value. This calculation based on wind speed frequencies accounts for the nonlinear dependence of gas flux terms on wind speed, which a monthly averaged wind speed would not. The wind speed and Liang et al. (2013)-derived value for $k_c/(k_{s,660} + k_{p,660})$ is 0.005–0.006 mol m^{-3}, which indicates that a measurable small bubble flux is necessary to account for the noble gas measurements and thus agrees more closely with the results that include diffusive gas exchange using a quasi steady state (equation (3)). The wind speed-determined small bubble term is lower than that determined from the noble gas data and equation (3) (0.010 ± 0.002 mol m^{-3}), likely indicating that the quasi steady state model overestimates the importance of small bubble fluxes. While the exposure of deep waters to the surface over several winters in a site like the Labrador Sea allows gases to approach a quasi steady state, it is reasonable to expect that a true steady state is not achieved before the deep mixed layer is isolated from the atmosphere. In regions with shallower winter mixed layers, a quasi steady state may be achieved allowing noble gases to act as an effective test of competing gas exchange parameterizations.

6. Predicting Other Gases

We can predict the impact of physical processes on other gases by writing equation (2) or (3) for another gas and solving for its saturation anomaly. One goal of our noble gas work is to predict physical background levels of the N_2/Ar ratio from which biological N_2 from denitrification can be distinguished. In the central Labrador Sea, oxygen levels are too high for water column denitrification, and benthic denitrification is largely confined to the shelves and boundary currents (Bianchi et al., 2012), so here we can use N_2/Ar measurements to test our prediction technique.

Including diffusive gas exchange strongly affects predictions of physical ΔN_2/Ar (Figure 4a). The mean of ΔN_2/Ar predictions for deep waters was $0.36 \pm 0.22\%$ for the first case excluding diffusive gas exchange and $1.18 \pm 0.36\%$ for the second case at quasi steady state. Observations average at $0.83 \pm 0.11\%$, between the two cases but closer to the quasi steady state, illustrating the impact of diffusive gas exchange in driving

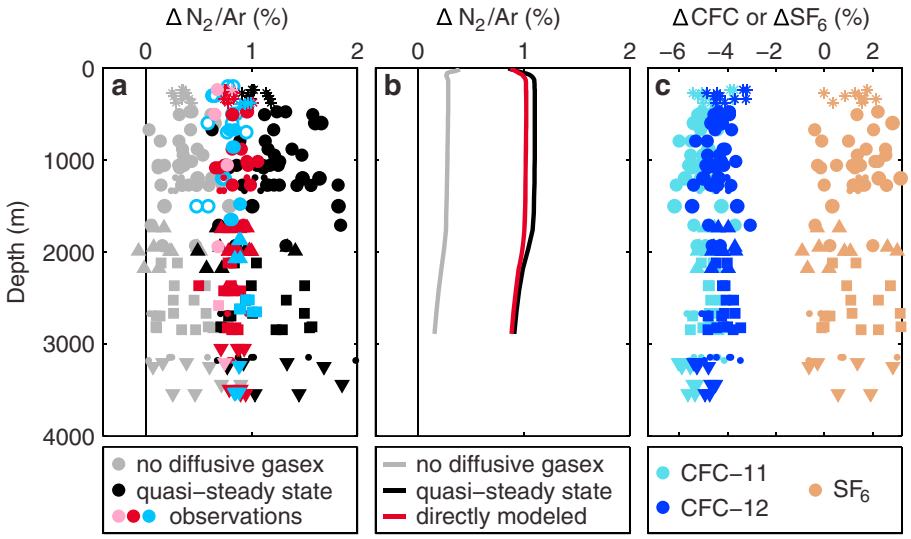

Figure 4. (a) Colored points indicate $\Delta N_2/Ar$ observations (same symbols as Figure 1). Gray points indicate $\Delta N_2/Ar$ predictions from the first case excluding diffusive gas exchange (equation (2). Black points indicate $\Delta N_2/Ar$ predictions from the second case based on a quasi steady state (equation (3). (b) Colored line indicates directly simulated $\Delta N_2/Ar$ in the Labrador Sea in the CESM. Gray and black lines indicate predictions of $\Delta N_2/Ar$ based on simulated noble gases. (c) Predictions of CFC-11, CFC-12, and SF_6 saturation anomalies if these gases had constant atmospheric levels, based on a quasi steady state.

ocean gas saturation anomalies. N_2 is half as soluble as Ar, so small bubble dissolution strongly supersaturates $\Delta N_2/Ar$ (Hamme & Emerson, 2013). This tracer highlights the difference in the importance of small bubbles between the two cases (Figure 3) and is consistent with the suggestion that the quasi steady state model overemphasizes the importance of small bubble processes.

We test our technique using inert gas distributions simulated in CESM. We solved equations (2) and (3) for the gas-independent terms using simulated Ne, Ar, and Kr and then predicted $\Delta N_2/Ar$. In Labrador Sea Water, predicted $\Delta N_2/Ar$ values were very similar to those predicted from our noble gas observations, 0.28% without diffusive gas exchange, and 1.10% for the quasi steady state (Figure 4b). Directly simulated $\Delta N_2/Ar$ values of 1.02% fall close to the quasi steady state prediction.

We can also predict the physically driven saturation anomalies of CFCs and SF_6. Recently, Stöven et al. (2016) suggested that bubble dissolution might explain elevated SF_6 measurements. Our predictions do not capture the time-dependent evolution of these transient tracers but do provide insight into time-independent physical processes. We predicted CFC-11, CFC-12, and SF_6 saturation anomalies as if these gases had constant atmospheric concentrations. All three gases have very temperature-dependent solubilities, more than twice Kr's. CFC-11 and CFC-12 are both quite soluble, so less affected by small bubble dissolution, whereas SF_6 is even less soluble than Ne, so strongly affected by small bubbles. Our calculations based on a quasi steady state show that SF_6 in Labrador Sea Water would be 6.2 and 6.8 % more supersaturated than CFC-12 and CFC-11, respectively, if these gases had constant atmospheric levels. While likely not a big enough difference to explain the large discrepancies in Stöven et al. (2016), such differences should be considered in transient tracer calculations.

7. Conclusions

Noble gas observations provide a powerful means to quantify the effect of physical processes on dissolved gases and to separate biological from physical impacts on gases like oxygen, nitrogen, and carbon. A quasi steady state that balances bubble fluxes, temperature change, atmospheric pressure change, and diffusive gas exchange better describes noble gas observations in the Labrador Sea than a model excluding diffusive gas exchange. This conclusion is supported by both the comparison between observed N_2/Ar and that predicted by the noble gas observations in a quasi steady state and by the correspondence between small bubble fluxes evaluated from the noble gas observations and those calculated from the wind speed parameterization of Liang et al. (2013). The technique of Loose et al. (2016), neglecting diffusive gas exchange, does not

yield realistic solutions with our data set. In the Labrador Sea, winter atmospheric pressures vary widely, so we must solve for this term in combination with large bubble fluxes, rather than a priori correcting gas saturation anomalies for atmospheric pressure. Alternatively, the temperature and bubble terms can be solved for using gas ratios, which are not affected by atmospheric pressure, and this approach yields the same result as our technique. The model that best fits the noble gas distributions suggests that the preformed saturation anomaly expected for SF_6 is ~6% higher than that of CFC-11 or CFC-12 in the Labrador Sea. The largest uncertainty in our work is the extent to which deeply convecting water exposed to the atmosphere over multiple winters reaches quasi steady state before winter's end. Applying our techniques to measurements from water mass formation regions with shallower winter mixed layers should be even more effective and may allow evaluation of competing gas exchange parameterizations.

Acknowledgments
We thank Karina Giesbrecht, Hollie Johnson, Charles Stump, Amanda Timmerman, Mariela White, and Mitchell Wolf for sample collection and analysis. We appreciate the support of scientists and technicians at the Fisheries and Oceans Canada Bedford Institute of Oceanography, especially Kumiko Azetsu-Scott, Ross Hendry, Stephen Punshon, and Marc Ringuette and the captains and crews of the CCGS Hudson and Amundsen. We thank Keith Lindsay for development and application of the CESM fast spin-up technique and Toste Tanhua for suggesting the CFC and SF_6 calculation. Data in this paper can be found at http://web.uvic.ca/~rhamme/download.html and at http://www.bco-dmo.org. The model output is available on the Earth System Grid (http://www.earthsystemgrid.org). NCEP Reanalysis data are provided by NOAA/OAR/ESRL PSD, Boulder, Colorado, USA, from their web site at http://www.esrl.noaa.gov/psd/. CCMP Version-2.0 analyses are produced by Remote Sensing Systems and sponsored by NASA Earth Science funding. Data are available at www.remss.com. This work was supported by NSERC DG 328290-2006 and 329290-2012 to R. Hamme, US NSF OCE-1029299 to S. Emerson, and NSERC CCARs 433898-2012 to Paul Myers and 433848-2012 to Roger Francois.

References

Aeschbach-Hertig, W., Peeters, F., Beyerle, U., & Kipfer, R. (2000). Palaeotemperature reconstruction from noble gases in ground water taking into account equilibration with entrapped air. *Nature*, *405*(6790), 1040–1044. https://doi.org/10.1038/35016542

Atlas, R., Hoffman, R. N., Ardizzone, J., Leidner, S. M., Jusem, J. C., Smith, D. K., & Gombos, D. (2011). A cross-calibrated, multiplatform ocean surface wind velocity product for meteorological and oceanographic applications. *Bulletin of the American Meteorological Society*, *92*, 157–174. https://doi.org/10.1175/2010BAMS2946.1

Beaird, N., Straneo, F., & Jenkins, W. (2015). Spreading of Greenland meltwaters in the ocean revealed by noble gases. *Geophysical Research Letters*, *42*, 7705–7713. https://doi.org/10.1002/2015GL065003

Bianchi, D., Dunne, J. P., Sarmiento, J. L., & Galbraith, E. D. (2012). Data-based estimates of suboxia, denitrification, and N_2O production in the ocean and their sensitivities to dissolved O_2. *Global Biogeochemical Cycles*, *26*, GB2009. https://doi.org/10.1029/2011GB004209

Bullister, J. L., Wisegarver, D. P., & Menzia, F. A. (2002). The solubility of sulfur hexafluoride in water and seawater. *Deep Sea Research Part I*, *49*(1), 175–187. https://doi.org/10.1016/S0967-0637(01)00051-6

Chang, B. X., Devol, A. H., & Emerson, S. R. (2012). Fixed nitrogen loss from the eastern tropical North Pacific and Arabian Sea oxygen deficient zones determined from measurements of N_2:Ar. *Global Biogeochemical Cycles*, *26*, GB3030. https://doi.org/10.1029/2011GB004207

Craig, H., & Weiss, R. F. (1971). Dissolved gas saturation anomalies and excess helium in the ocean. *Earth and Planetary Science Letters*, *10*(3), 289–296. https://doi.org/10.1016/0012-821X(71)90033-1

Danabasoglu, G., Bates, S. C., Briegleb, B. P., Jayne, S. R., Jochum, M., Large, W. G., … Yeager, S. G. (2012). The CCSM4 ocean component. *Journal of Climate*, *25*(5), 1361–1389. https://doi.org/10.1175/JCLI-D-11-00091.1

Emerson, S., & Bushinsky, S. (2016). The role of bubbles during air-sea gas exchange. *Journal of Geophysical Research: Oceans*, *121*, 4360–4376. https://doi.org/10.1002/2016JC011744

Emerson, S., Ito, T., & Hamme, R. C. (2012). Argon supersaturation indicates low decadal-scale vertical mixing in the ocean thermocline. *Geophysical Research Letters*, *39*, L18610. https://doi.org/10.1029/2012GL053054

Emerson, S., Stump, C., Wilbur, D., & Quay, P. (1999). Accurate measurement of O_2, N_2, and Ar gases in water and the solubility of N_2. *Marine Chemistry*, *64*(4), 337–347. https://doi.org/10.1016/S0304-4203(98)00090-5

Hamme, R. C., & Emerson, S. R. (2002). Mechanisms controlling the global oceanic distribution of the inert gases argon, nitrogen and neon. *Geophysical Research Letters*, *29*(23), 2120. https://doi.org/10.1029/2002GL015273

Hamme, R. C., & Emerson, S. R. (2004). The solubility of neon, nitrogen and argon in distilled water and seawater. *Deep Sea Research Part I: Oceanographic Research Papers*, *51*(11), 1517–1528. https://doi.org/10.1016/j.dsr.2004.06. 009

Hamme, R. C., & Emerson, S. R. (2006). Constraining bubble dynamics and mixing with dissolved gases: Implications for productivity measurements by oxygen mass balance. *Journal of Marine Research*, *64*(1), 73–95. https://doi.org/10.1357/002224006776412322

Hamme, R. C., & Emerson, S. R. (2013). Deep-sea nutrient loss inferred from the marine dissolved N_2/Ar ratio. *Geophysical Research Letters*, *40*, 1149–1153. https://doi.org/10.1002/grl.50275

Hamme, R. C., & Severinghaus, J. P. (2007). Trace gas disequilibria during deep-water formation. *Deep Sea Research Part I: Oceanographic Research Papers*, *54*(6), 939–950. https://doi.org/10.1016/j.dsr.2007.03.008

Hohmann, R., Schlosser, P., Jacobs, S., Ludin, A., & Weppernig, R. (2002). Excess helium and neon in the southeast Pacific: Tracers for glacial meltwater. *Journal of Geophysical Research*, *107*(C11), 3198. https://doi.org/10.1029/2000JC000378

Holland, M. M., Bailey, D. A., Briegleb, B. P., Light, B., & Hunke, E. (2012). Improved sea ice shortwave radiation physics in CCSM4: The impact of melt ponds and aerosols on Arctic sea ice. *Journal of Climate*, *25*(5), 1413–1430. https://doi.org/10.1175/JCLI-D-11-00078.1

Hunke, E., & Lipscomb, W. (2008). CICE: The Los Alamos sea ice model, documentation and software user's manual, version 4.0 (Tech. Rep. LA-CC-06-012). Los Alamos National Laboratory.

Hurrell, J. W., Holland, M. M., Gent, P. R., Ghan, S., Kay, J. E., Kushner, P. J., … Marshall, S. (2013). The Community Earth System Model: A framework for collaborative research. *Bulletin of the American Meteorological Society*, *94*(9), 1339–1360. https://doi.org/10.1175/BAMS-D-12-00121.1

Ito, T., & Deutsch, C. (2006). Understanding the saturation state of argon in the thermocline: The role of air-sea gas exchange and diapycnal mixing. *Global Biogeochemical Cycles*, *20*, GB3019. https://doi.org/10.1029/2005GB002655

Ito, T., Hamme, R. C., & Emerson, S. (2011). Temporal and spatial variability of noble gas tracers in the North Pacific. *Journal of Geophysical Research*, *116*, C08039. https://doi.org/10.1029/2010JC006828

Kalnay, E., Kanamitsu, M., Kistler, R., Collins, W., Deaven, D., Gandin, L., … Joseph, D. (1996). The NCEP/NCAR 40-year reanalysis project. *Bulletin of the American Meteorological Society*, *77*(3), 437–471. https://doi.org/10.1175/1520-0477(1996)077<0437:TNYRP>2.0.CO;2

Kay, J. E., Deser, C., Phillips, A., Mai, A., Hannay, C., Strand, G., … Vertenstein, M. (2014). The Community Earth System Model (CESM) large ensemble project: A community resource for studying climate change in the presence of internal climate variability. *Bulletin of the American Meteorological Society*, *96*, 1333–1349. https://doi.org/10.1175/BAMS-D-13-00255.1

Kobashi, T., Severinghaus, J. P., & Kawamura, K. (2008). Argon and nitrogen isotopes of trapped air in the GISP2 ice core during the Holocene epoch (0–11,500 B.P.): Methodology and implications for gas loss processes. *Geochimica et Cosmochimica Acta*, *72*(19), 4675–4686. https://doi.org/10.1016/j.gca.2008.07.006

Liang, J.-H., Deutsch, C., McWilliams, J. C., Baschek, B., Sullivan, P. P., & Chiba, D. (2013). Parameterizing bubble-mediated air-sea gas exchange and its effect on ocean ventilation. *Global Biogeochemical Cycles*, *27*(3), 894–905. https://doi.org/10.1002/gbc.20080

Lindsay, K. (2017). A Newton-Krylov solver for fast spin-up of online ocean tracers. *Ocean Modeling*, *109*, 33–43. https://doi.org/10.1016/j.ocemod.2016.12.001

Long, M. C., Lindsay, K., Peacock, S., Moore, J. K., & Doney, S. C. (2013). Twentieth-century oceanic carbon uptake and storage in CESM1(BGC). *Journal of Climate*, *26*(18), 6775–6800. https://doi.org/10. 1175/JCLI-D-12-00184.1

Long, M. C., Deutsch, C., & Ito, T. (2016). Finding forced trends in oceanic oxygen. *Global Biogeochemical Cycles*, *30*, 381–397. https://doi.org/10.1002/2015GB005310

Loose, B., Jenkins, W. J., Moriarty, R., Brown, P., Jullion, L., Naveira Garabato, A. C., … Meredith, M. P. (2016). Estimating the recharge properties of the deep ocean using noble gases and helium isotopes. *Journal of Geophysical Research: Oceans*, *121*, 5959–5979. https://doi.org/10.1002/2016JC011809

Myers, P. G. (2005). Impact of freshwater from the Canadian Arctic Archipelago on Labrador Sea water formation. *Geophysical Research Letters*, *32*, L06605. https://doi.org/10.1029/2004GL022082

NASA (1976). *US Standard Atmosphere, 1976*. Washington, DC: US Government Printing Office.

Nicholson, D., Emerson, S., Caillon, N., Jouzel, J., & Hamme, R. C. (2010). Constraining ventilation during deepwater formation using deep ocean measurements of the dissolved gas ratios $^{40}Ar/^{36}Ar$, N_2/Ar, and Kr/Ar. *Journal of Geophysical Research*, *115*, C11015. https://doi.org/10.1029/2010JC006152

Nicholson, D., Khatiwala, S., & Heimbach, P. (2016). Noble gas tracers of ventilation during deep-water formation in the Weddell Sea. *IOP Conference Series: Earth and Environmental Science*, *35*, 012019, IOP Publishing. https://doi.org/10.1088/1755-1315/35/1/012019

Postlethwaite, C., Rohling, E., Jenkins, W., & Walker, C. (2005). A tracer study of ventilation in the Japan/East Sea. *Deep Sea Research Part II*, *52*(11–13), 1684–1704. https://doi.org/10.1016/j.dsr2.2004.07.032

Smith, R. D., Jones, P., Bryan, F., Danabasoglu, G., Dennis, J., Dukowicz, J., … Yeager, S. (2010). The Parallel Ocean Program (POP) reference manual (Tech. Rep. LAUR-10-01853). Los Alamos National Laboratory. Retrieved from http://www.cesm.ucar.edu/models/cesm1.0/pop2/doc/sci/POPRefManual.pdf

Spitzer, W. S., & Jenkins, W. J. (1989). Rates of vertical mixing, gas exchange and new production: Estimates from seasonal gas cycles in the upper ocean near Bermuda. *Journal of Marine Research*, *47*(1), 169–196. https://doi.org/10.1357/002224089785076370

Stanley, R. H., & Jenkins, W. J. (2013). Noble gases in seawater as tracers for physical and biogeochemical ocean processes. In R. H. Stanley & W. J. Jenkins (Eds.), *The Noble Gases as Geochemical Tracers* (pp. 55–79). New York: Springer. https://doi.org/10.1007/978-3-642-28836-4_4

Stanley, R. H., Jenkins, W. J., Lott, D. E., & Doney, S. C. (2009). Noble gas constraints on air-sea gas exchange and bubble fluxes. *Journal of Geophysical Research*, *114*, C11020. https://doi.org/10.1029/2009JC005396

Stöven, T., Tanhua, T., Hoppema, M., & von Appen, W.-J. (2016). Transient tracer distributions in the Fram Strait in 2012 and inferred anthropogenic carbon content and transport. *Ocean Science*, *12*(1), 319–333. https://doi.org/10.5194/os-12-319-2016

Sturm, P., Leuenberger, M., Sirignano, C., Neubert, R., Meijer, H., Langenfelds, R., … Tohjima, Y. (2004). Permeation of atmospheric gases through polymer O-rings used in flasks for air sampling. *Journal of Geophysical Research*, *109*, D04309. https://doi.org/10.1029/2003JD004073

Stute, M., Schlosser, P., Clark, J. F., & Broecker, W. S. (1992). Paleotemperatures in the southwestern United States derived from noble gases in ground water. *Science*, *256*(5059), 1000–1003.

Toggweiler, J. R., Gnanadesikan, A., & Carson, S. (2003). Representation of the carbon cycle in box models and GCMs: 1. Solubility pump. *Global Biogeochemical Cycles*, *17*(1), 1026. https://doi.org/10.1029/2001GB001401

Wanninkhof, R. (1992). Relationship between wind speed and gas exchange over the ocean. *Journal of Geophysical Research*, *97*(C5), 7373–7382. https://doi.org/10.1029/92JC00188

Warner, M., & Weiss, R. (1985). Solubilities of chlorofluorocarbons 11 and 12 in water and seawater. *Deep Sea Research Part A, Oceanographic Research Papers*, *32*(12), 1485–1497. https://doi.org/10.1016/0198-0149(85)90099-8

Weiss, R. F., & Kyser, T. K. (1978). Solubility of krypton in water and seawater. *Journal of Chemical and Engineering Data*, *23*(1), 69–72. https://doi.org/10.1021/je60076a014

Yashayaev, I. (2007). Hydrographic changes in the Labrador Sea, 1960–2005. *Progress in Oceanography*, *73*(3–4), 242–276. https://doi.org/10.1016/j.pocean.2007.04.015

Yashayaev, I., & Loder, J. W. (2016). Recurrent replenishment of Labrador Sea water and associated decadal-scale variability. *Journal of Geophysical Research: Oceans*, *121*, 8095–8114. https://doi.org/10.1002/2016JC012046